

# Contents

## Introduction

- Multicrystal, real microstructures
- Cubic meshes
- Polycrystal aggregates, realistic microstructures

## Aggregate

- Mesh generation
- Convergence tests
- Effect of the boundary conditions
- Intragranular response

# FE calculations of crystalline microstructures

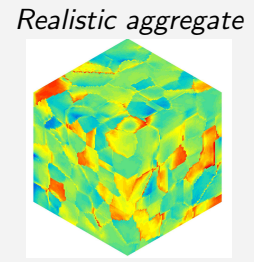
Georges Cailletaud

Centre des Matériaux  
Ecole des Mines de Paris/CNRS

# Computations at various scales



Level (1)  
Macroscopic models  
Average stress and strain tensor



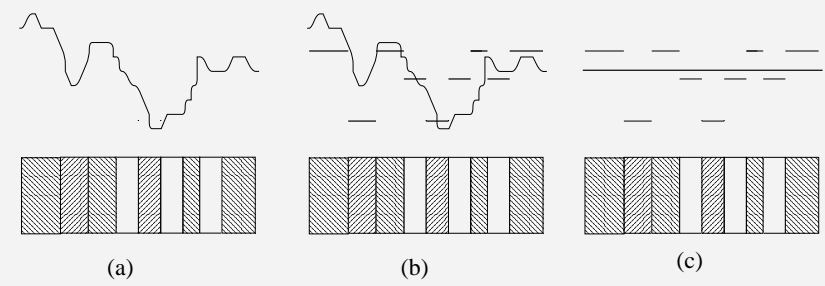
Level (3)  
Local information  
Respect local Constitutive Equations  
Equilibrium

Intermediate level  
Averaging process  
(2) phase by phase  
(2') grain by grain

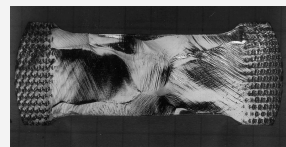
Level (2) or (2')  
Local average  
Respect local Constitutive Equations  
no neighboring effect

# Various scales in heterogeneous material modeling

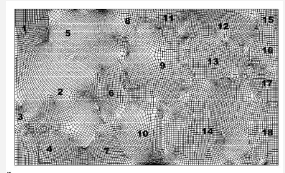
- (a) Microstructure calculation: take into account local phases and local equilibrium (This lecture)
- (b) Uniform field models: take into account local phases only
- (c) Macroscopic models: do not account for local phases nor local equilibrium



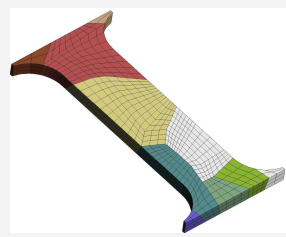
# Multicrystals, real microstructures



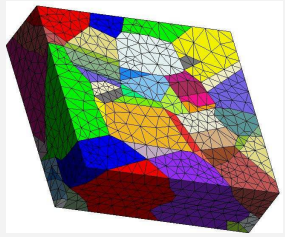
[Delaire et al., 2000]



[Raabe et al., 1981]

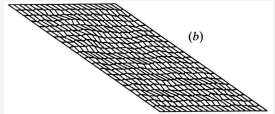
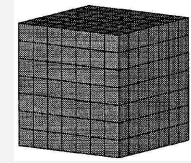
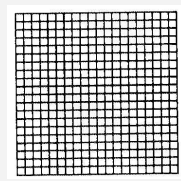


[Eberl et al., 1998]



Next lecture

# Cubic meshes, cube elements



2D  
[Kalidindi et al., 1992]



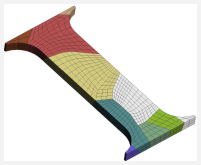
3D  
[Miehe et al., 1999]

Meshes used for homogenization purpose

# Various types of FE computations using crystal plasticity

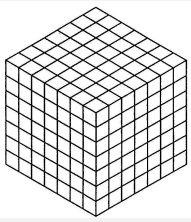
Single Crystal models in each Gauss point

Multicrystals



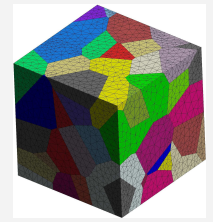
Real specimens  
with a few grains  
to check local fields  
With experiments

Cubic meshes



Cubes  
1 grain/elt  
Numerical  
Homogenization

Polycrystal aggregates



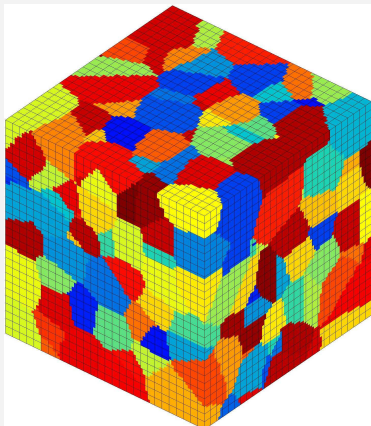
Realistic microstructures  
Many Gauss Pt/grain  
Homogenization  
AND Relocalization

# State-of-the-art on real microstructures

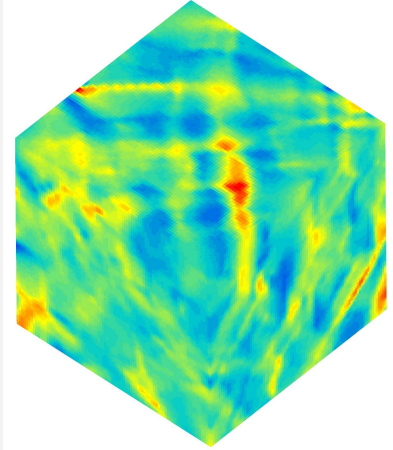
- Good agreement, specially for large grains
- Problems near grain boundaries
- Behavior of a grain in its environment  $\neq$  single crystal behavior
- Primary–secondary slip
- Problem surface–volume (2D–3D meshes ?)
- Example of a OFHC copper specimen, coming...

# Polycrystal aggregates

Work by Barbe (2000), Diard (2002), Musienko (2005)

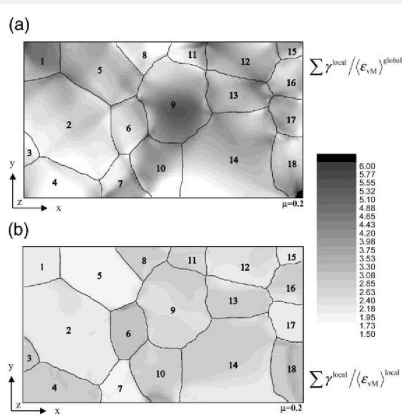


28x28x28 mesh



Local field of total axial strain

# Influence of GB's



Global and local Taylor factor

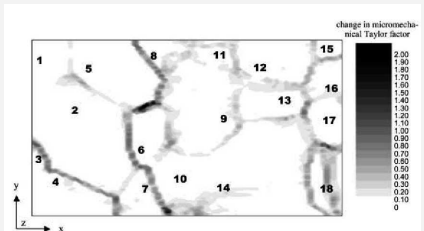
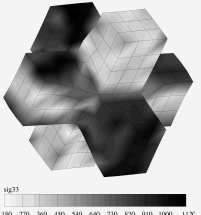
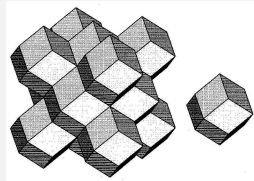
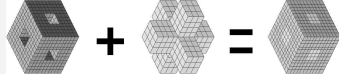


Illustration of the perturbation due to grain boundary by the variation of the local Taylor factor

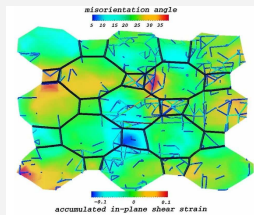
It is noteworthy that the grain boundary from 20 to 100 micrometers length area (shown in Fig. 20) is affected by the grain boundary perturbation. The grain boundary from 20 to 100 micrometers length area is affected by grain boundary perturbation. The grain boundary from 20 to 100 micrometers length area is affected by grain boundary perturbation. The grain boundary from 20 to 100 micrometers length area is affected by grain boundary perturbation.

(more in [Raabe et al., 1981])

# Polycrystalline aggregates (2)

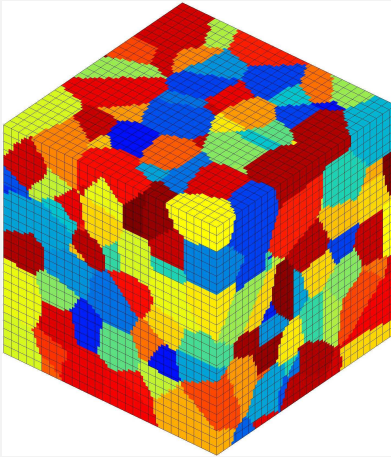


[Bugat et al., 1999]  
Looking for level (2) info

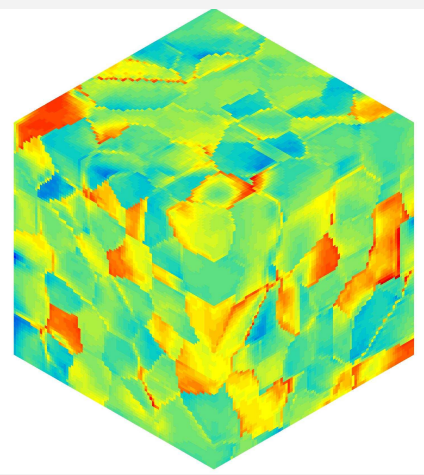


[Mika and Dawson, 1999]  
Looking for level (3) info

# Polycrystal aggregates



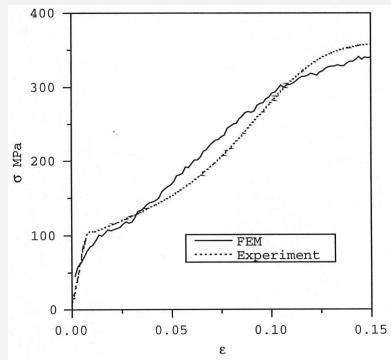
28x28x28 mesh



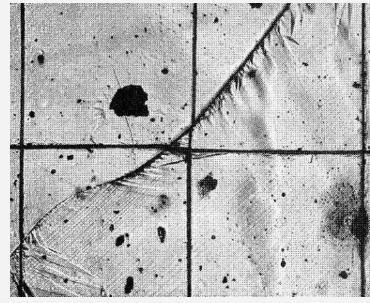
Local field of von Mises stress

# Slip and twinning in Magnesium

(more in [Staroselski and Anand, 2003])



Compression on AZ31 works only with GB model

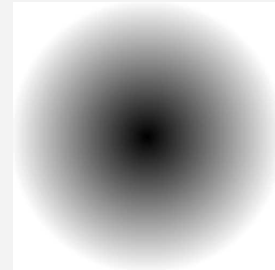


Hauser (1955)

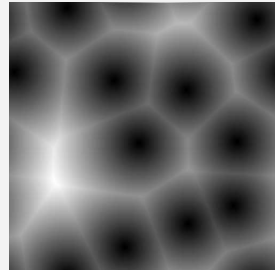
Slip system contribution + von Mises for GB's

$$\underline{\underline{L}}^P = (1 - \xi) \sum_s \hat{\gamma}^s \text{sign}(\tau^s) \underline{\underline{S}}_0^s + \xi \underline{\underline{M}}$$

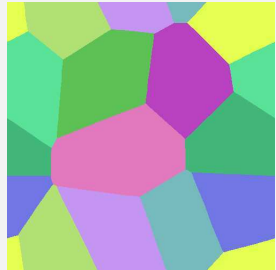
# Construction of Voronoï polyhedra



Distance function of a single point source

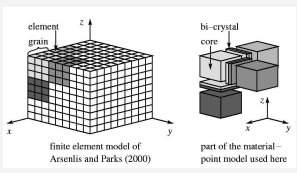


Distance function of a set of point sources

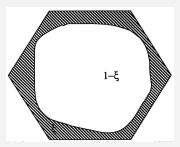


Final result after construction and labelling

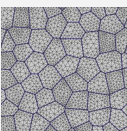
# A need for Grain Boundaries



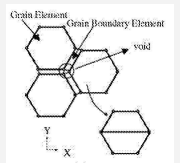
[Evers et al., 2002]



[Staroselski and Anand, 2003]



[Cailletaud et al., 2002]

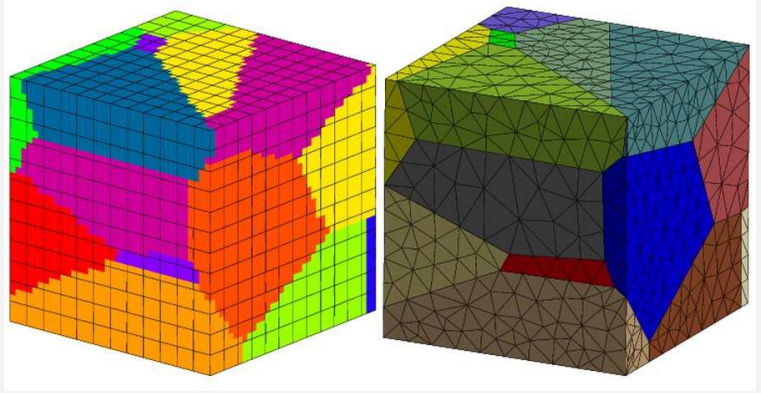


[Kim et al., 2002]

# State-of-the-art on cubic meshes and RVEs

- Periodic cells – Polycrystal RVE
- Generally rather good for texture prediction, not so far from Taylor (too stiff)
- Representative provided 200–300 grains are used
- Validity of the local information on approximative geometries ?
- Realistic morphologies are necessary to capture local stress and strain fields

### Typical realization and the associated meshes

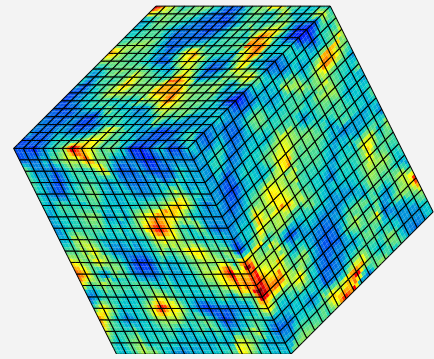


Multiphase element technique

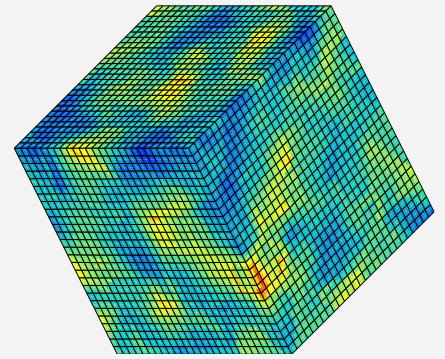
Real 3D mesh respecting grain boundaries

### Effect of the FE interpolation

- Comparison between two strategies with 157464 integration points



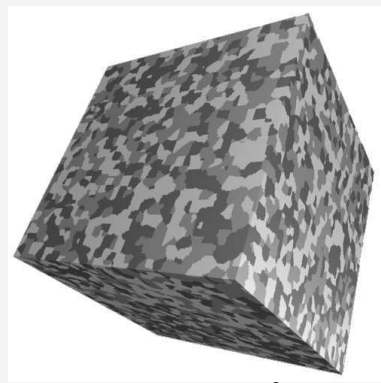
$18^3 = 5832$  quadratic elts



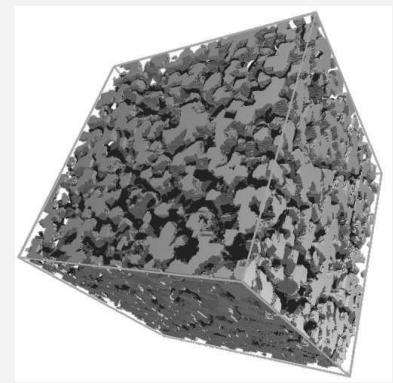
$27^3 = 19683$  linear elts

Contour of accumulated slip after 0.015 extension

### Example of a three phase material with 16000 grains



Cubic domain of  $250^3$  voxels



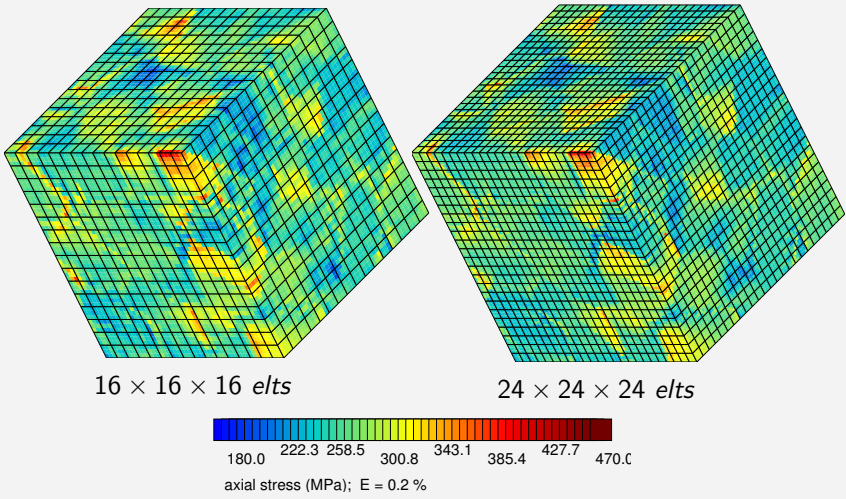
3D view  
Extraction of phase 1

### Tests on various FE configurations

- Effect of the orientation distribution
  - Number of grains
  - Number of Euler angle sets
  - 200 grains or more, randomly distributed
- Effect of the FE interpolation
  - quadratic interpolation, full integration
- Effect of mesh size
  - 16 for macro, much more for local...

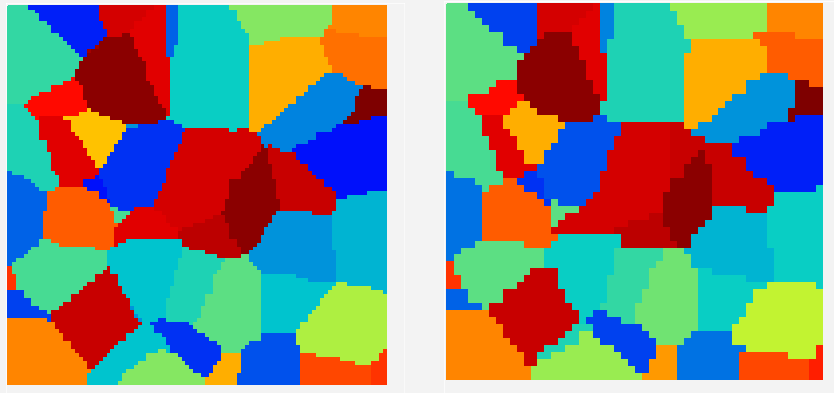
Tests made in tension, with  $\underline{\epsilon} = \text{Diag}(\epsilon, -0.5\epsilon, -0.5\epsilon)$

### Effect of the mesh size on local stress field



Quadratic mesh, axial tension 0.2%, 200 grains

### Effect of the mesh size: geometry



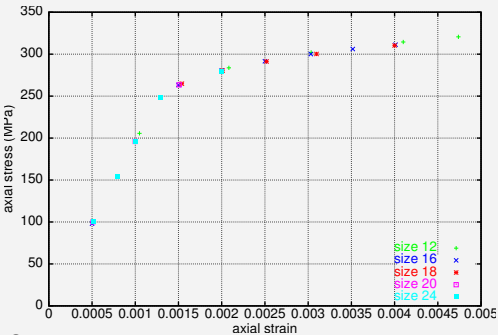
32 x 32 x 32 elts

18 x 18 x 18 elts

Quadratic mesh, axial tension, 200 grains

### Effect of the mesh size

#### Global response



Stress – strain curve

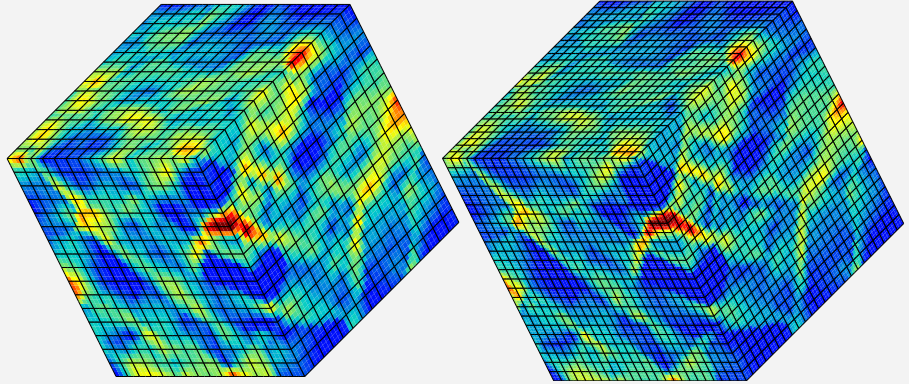
#### Local response

elt number	min	max
12 <sup>3</sup>	194.80	411.02
16 <sup>3</sup>	191.42	464.42
18 <sup>3</sup>	185.68	456.90
20 <sup>3</sup>	184.19	470.94
24 <sup>3</sup>	180.37	470.91

Min and Max local values of the axial stress

Pure extension to  $\epsilon_{zz} = 0.015$

### Effect of the mesh size on accumulated plastic strain



16 x 16 x 16 elts

24 x 24 x 24 elts

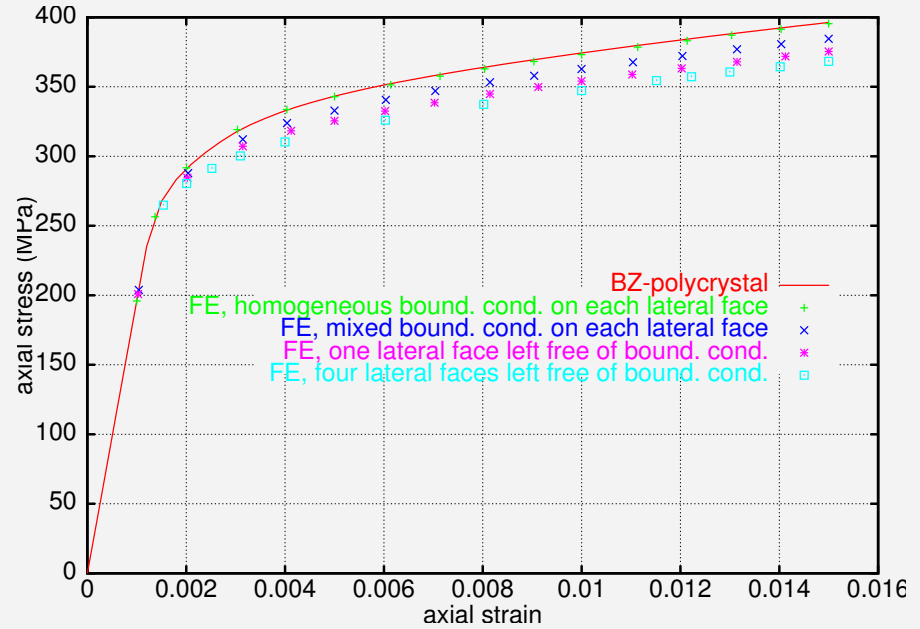
Quadratic mesh, axial tension 0.2%, 200 grains

# The problem of the boundary conditions

- From homogenization theory:
  - The macroscopic response of a RVE should be independent of boundary conditions
- Four boundary conditions have been used
  - HSB Homogeneous Strain at the Boundary: full constraint
  - MB Mixed Boundary condition: flat lateral faces
  - 1FF 1 Free Face
  - 4FF 4 Free Faces

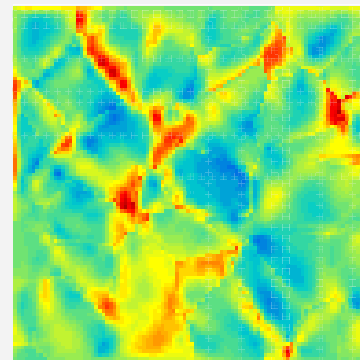
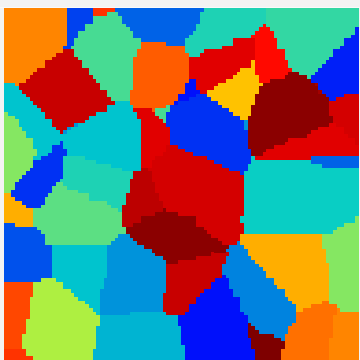
Tests made in pure tension, trying to keep a zero lateral force

# Macroscopic responses: axial stress–strain curves



Homogeneous strain BC present the best agreement with BZ model

# Effect of the mesh size on accumulated plastic strain



range: 0.003 – 0.089

Geometry

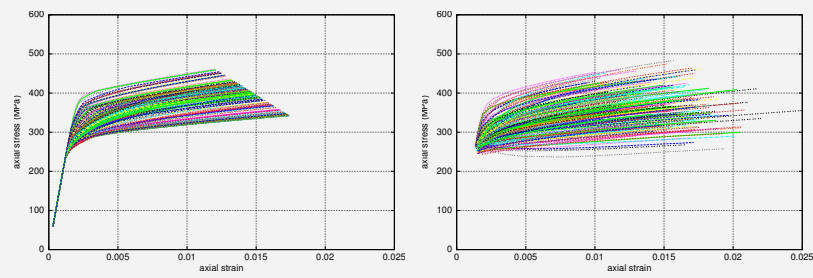
32 × 32 × 32 elts

Quadratic mesh, axial tension 0.2%, 200 grains

# Effect of the boundary conditions

- Low on the macroscopic response (level 1)
  - Self-consistent model in good agreement with FE
- Significant on the mean value in the grain (level 2)
  - More scatter in FE than in self-consistent approach
  - More scatter in terms of stress for HSB
  - More scatter in terms of strain for 4FF
- Very high on intragranular fields (level 3)
  - Stress and strain gradients inside the grains

# Grain responses: axial stress–strain curves

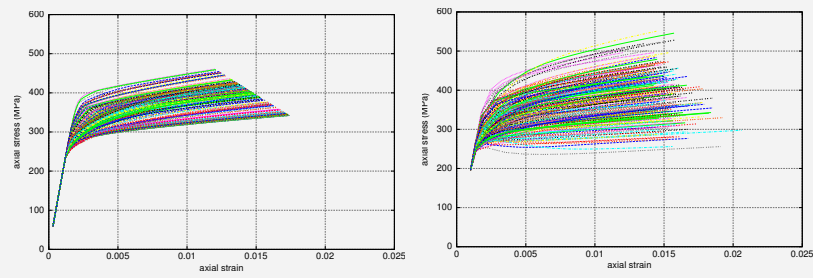


Self-consistent model

4 free faces

Axial  $\sigma$ - $\epsilon$  curves , tension to  $\epsilon_{zz} = 0.015$

# Grain responses: axial stress–strain curves



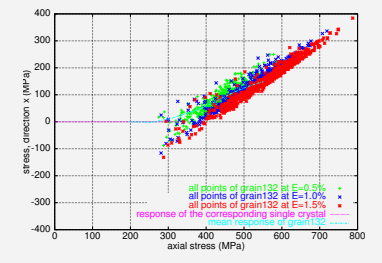
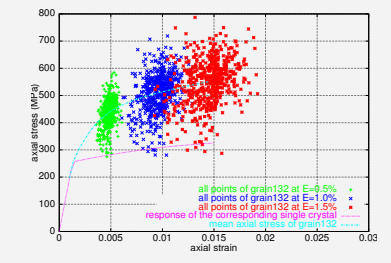
Self-consistent model

Homogeneous strain BC

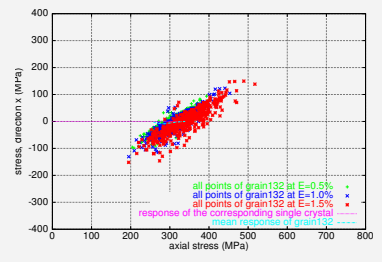
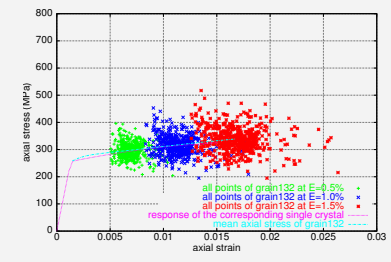
Axial  $\sigma$ - $\epsilon$  curves , tension to  $\epsilon_{zz} = 0.015$

# Local response of the strongest grain

## Homogeneous strain



## 4 Free Faces

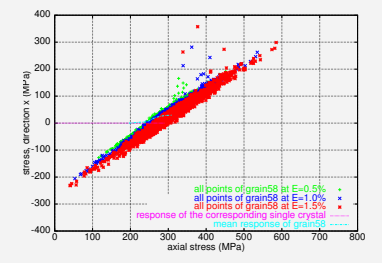
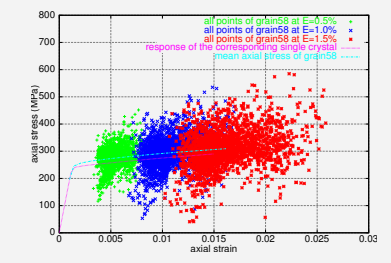


Axial stress-strain curve

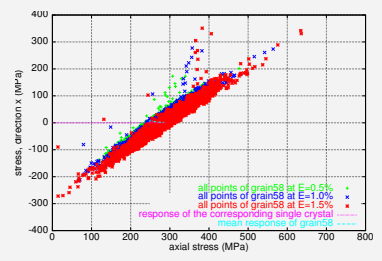
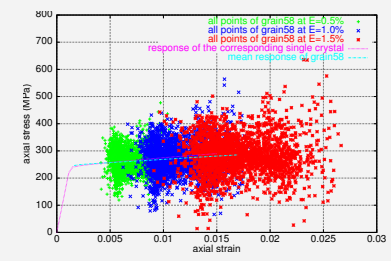
Lateral versus axial stress

# Local response of the biggest grain

## Homogeneous strain



## 4 Free Faces

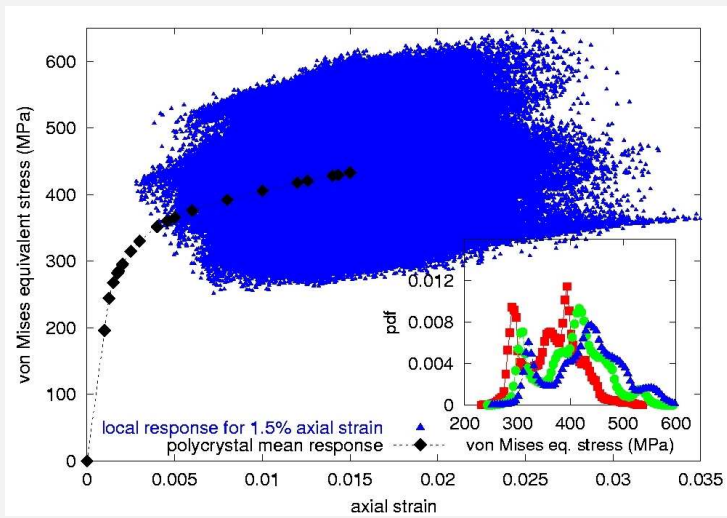


Axial stress-strain curve

Lateral versus axial stress



## A result on all the Gauss points in the cube



Two populations ?

34 / 40

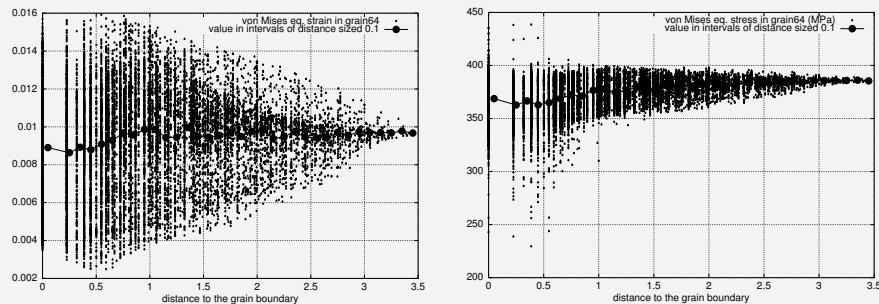
## Parallel computations



- ZéBuLoN FE code
- Z-mat material library
- Computations on a linux PC cluster
- FETI method for parallel computation (with Onera/Feyel)
- August 2006: 160 64-bit processors

36 / 40

## Scatter due to grain boundary (GB)



Equivalent plastic strain  
versus dist to the GB

Equivalent stress (von Mises)  
versus dist to the GB






33 / 40

## Perspectives






- Provide information for the higher level
- Take information from lower level
- Use finer and finer meshes (parallel computing)
- Change the crystallographic model (HCP, next lecture )
- Introduce damage (intergranular damage and cleavage, next lecture )
- Use in stress/strain fields presenting strong gradients, for instance with Cosserat type models, not shown here (see for instance [Forest et al., 2000] )

more in [Barbe et al., 2001a, Barbe et al., 2001b, Barbe et al., 2003]  
[Cordier et al., 2005]

35 / 40


-  [Cordier, P., Barbe, F., Durinck, J., Tommasi, A., and Walker, A. \(2005\).](#)  
Plastic Deformation of mantle minerals: Multiscale numerical modelling, volume 7 of EMU Notes in Mineralogy, chapter 1, pages 1–42.
-  [Delaire, F., Raphanel, J., and Rey, C. \(2000\).](#)  
Plastic heterogeneities of a copper multicrystal deformed in uniaxial tension: experimental study and finite element simulations. *Acta Metall.*, 48:1075–1087.
-  [Eberl, F., Feyel, F., Quilici, S., and Cailletaud, G. \(1998\).](#)  
*Approches numériques de la plasticité cristalline.* *J. de Physique IV*, 8:Pr4–15–Pr4–25.
-  [Evers, L., Parks, D., Brekelmans, W., and Geers, M. \(2002\).](#)  
Crystal plasticity model with enhanced hardening by geometrically necessary dislocation accumulation. *J. Mech. Phys. Sol.*, 50:2403–2424.
-  [Forest, S., Barbe, F., and Cailletaud, G. \(2000\).](#)  
Cosserat modelling of size effects in the mechanical behaviour of polycrystals and multiphase materials.

38 / 40






-  [Barbe, F., Decker, L., Jeulin, D., and Cailletaud, G. \(2001a\).](#)  
Intergranular and intragranular behavior of polycrystalline aggregates. Part I: FE model. *Int. J. of Plasticity*, 17(4):513–536.
-  [Barbe, F., Forest, S., and Cailletaud, G. \(2001b\).](#)  
Intergranular and intragranular behavior of polycrystalline aggregates. Part II: Results. *Int. J. of Plasticity*, 17(4):537–566.
-  [Barbe, F., Quilici, S., Forest, S., and cailletaud, G. \(2003\).](#)  
Numerical study of crystalline plasticity: measurements of the heterogeneities due to grain boundaries under small strains. *Revue de Métallurgie*, pages 815–823.
-  [Bugat, S., Besson, J., and Pineau, A. \(1999\).](#)  
Micromechanical modeling of the behavior of duplex stainless steels. *Computational Materials Science*, 16:158–166.
-  [Cailletaud, G., Diard, O., and Musienko, A. \(2002\).](#)  
Damage, opening and sliding of grain boundaries. *In et al., S. A., editor, Multiscale Modelling of Engng. Materials, Marrakech, Oct. 2002, pages 149–156. Kluüwer.*

37 / 40

*Micromechanical and macromechanical effects in grain scale polycrystal plasticity experimentation and simulation.* *Acta Metall.*, 49:3433–3441.

-  [Staroselski, A. and Anand, L. \(2003\).](#)  
A constitutive model for hcp materials deforming by slip and twinning: application to magnesium alloy az31b. *Int. J. of Plasticity*, 19:1843–1864.

*Int. J. Solids Structures*, 37:7105–7126.

-  [Kalidindi, S., Bronkhorst, C., and Anand, L. \(1992\).](#)  
Crystallographic texture evolution in bulk deformation processing of FCC metals. *J. Mech. Phys. Sol.*, 40:536–569.
-  [Kim, D., Ku, T., and Kang, B. \(2002\).](#)  
Finite element analysis of micro-rolling using grain and grain boundary elements. *J. of Materials Processing Technology*, 130–131:456–461.
-  [Miehe, C., Schröder, J., and Schotte, J. \(1999\).](#)  
Computational homogenization analysis in finite plasticity simulation of texture development in polycrystalline materials. *Comp. Meth. Appl. Mech. Engng*, 171:387–418.
-  [Mika, D. and Dawson, P. \(1999\).](#)  
Polycrystal plasticity modeling of intracrystalline boundary textures. *Acta Metall.*, 47:1355–1369.
-  [Raabe, D., Sachtler, M., Zhao, Z., Roters, F., and Zaefferer, S. \(1981\).](#)

40 / 40

39 / 40